



# Multi-objective optimal control with carbon emission and temperature constraints: for achieving a low-fossil-fuel economy

Helmut Maurer<sup>1</sup> · Willi Semmler<sup>2,3,4</sup> 

Accepted: 26 February 2025  
© The Author(s) 2025

## Abstract

In this paper we propose multi-objective control to deal with climate change and climate risks and the transition to a low carbon economy. Extending our previous collaborative work as in Atolia et al. (Math Control Related Fields, 13:583–604, 2023), we again build on the Nordhaus type DICE model to include various optimal macroeconomic policies such as mitigation, adaptation and climate-related infrastructure investment studying the dynamics of the decarbonizing of the economy. Based on a finite horizon model that includes the threats of climate disasters arising from  $CO_2$  emissions and temperature rise, we deal with preventive measures such as adaptation reducing disaster effects. Our optimal control problem of finite horizon is consisting of a dynamical system with five-dimensional state vector representing stocks of private capital, green capital, public capital, stock of brown energy in the ground, carbon emissions, and temperature. The objective function captures preferences over consumption but is also impacted by atmospheric  $CO_2$ , climate risks events and by mitigation and adaptation policies. Given the numerous challenges to climate change policies with multiple objectives the control vector is eight-dimensional including mitigation, adaptation and infrastructure investment. The optimal control problem is studied under various state constraints. In two scenarios we compute the Pareto front for a bi-objective control problem. Optimization over the Pareto front provides us with suitable weights for the two objectives. In particular we explore the role of  $CO_2$  constraints, as the Kyoto Protocol has suggested, and temperature constraints, as the Copenhagen–Paris agreements have proposed.

**Keywords** Climate change model · Mitigation · Optimal control · Discretization methods · Turnpike solution · Fiscal policy

**Mathematics Subject Classification** Primary 49N90 · 49K15 · 49M37; Secondary 91-08

---

H. Maurer and W. Semmler have contributed equally to this work.

---

Extended author information available on the last page of the article

## 1 Introduction

The Paris, December 2015, COP 20 agreement on climate change is aiming at reducing the temperature increase to below  $2^{\circ}\text{C}$  relative to pre-industrial level. This implies that effective mitigation policies need to be pursued that not only prevent the  $\text{CO}_2$  emission from rising further but should reduce the annual emission substantially. The Paris agreement is detailed in the IPCC (2018) report that demonstrates higher probability of limiting global warming to  $1.5^{\circ}\text{C}$  will only be obtained, if a significant reduction of  $\text{CO}_2$  net emissions from 2020 to 2040 will be achieved. From then on the upper bound of  $\text{CO}_2$  should not be exceeded anymore.

Since those upper limits create great policy challenges we propose here a modeling strategy that, attempts to answer three questions coming up in this context: First, what are the best strategies to keep the  $\text{CO}_2$  emission bounded by a predefined upper bound, and, correspondingly, how can one steer down the  $\text{CO}_2$  emission if it already has reached too high a level. Second, how can climate policies be scaled up and what resources should be allocated to mitigation and adaptation efforts, especially for the latter, in particular, when climate risk, due to a lack of emission reduction, is rising and future economic, social, and ecological damages can be expected. A third issue is of how the efforts of mitigation and adaptation are funded and how the funds should dynamically be allocated between traditional infrastructure investment, mitigation and adaptation efforts—and in what sequence.

A number of those issues have been studied in Integrated Assessment Models (IAMs) of various kind using scientific modelling to link the economy with the biosphere and the atmosphere. This broad class of IAMs focusing on economy-climate interaction, use various scientific modeling and estimation methods. In our paper we more specifically focus on the seminal work by Nordhaus (2008, 2017) on the economy-climate link. This work specifically introduces the economy-climate interaction in mathematical formulations of an economic growth model, integrating into the model of carbon emission from industrial production, damages from it affecting output, and an optimal mitigation policy. Nordhaus calls his major work a Dynamic Integrated Model of Climate and the Economy, in short a DICE model. For details of the DICE model, see Nordhaus and Boyer (2000) and Nordhaus (2008).

We extend the latter Nordhaus type model to include beside mitigation, optimal policies for adaptation and infrastructure investment exploring the dynamics of the transition to a low fossil-fuel economy. Since mitigation policy is mainly aiming at phasing in of renewable energy we also explore what amount of traditional fossil energy is allowed to be extracted when setting some carbon emission and temperature constraints. Whereas Nordhaus employs as objective function preferences over consumption, based on standard growth theory, our objective function captures multiple targets—preferences over consumption, but is also impacted by atmospheric  $\text{CO}_2$  as well as the mitigation and adaptation policies. Our dynamic model, as it includes the phasing in of renewable energy along with the issues mentioned above, can be considered an extension of the DICE type models.

We present a dynamic global model with feedback control, representing an optimal control, that allows us to consider the specific policies of infrastructure

investment, mitigation and adaptation. The model is micro-founded in the sense that we employ a production technology which uses (private) physical capital and energy as inputs. Labor input is suppressed for simplicity as it is supplied inelastically. There are two sources of energy: non-renewable, brown energy produced by an extractive resource sector and renewable, green energy produced with (private physical) green capital. The emissions from brown energy use are a source of negative externality that directly enters the (instantaneous) felicity function. Note that we do not make damages to households dependent on the temperature, but rather on the stock of emissions. The reason is that the time series data on temperature is very heterogeneous across regions and quite volatile over time.

In our model the government levies lump-sum taxes to raise revenues, a portion of which provides direct utility, another portion is invested in public (physical) capital, and remaining part is administrative expense. For models with other sources of capital, such as for example bond financing, see Bonen et al. (2016), and Orlov et al. (2018). The traditional use of public capital is to serve as infrastructure investment that augments the productivity of the production process. This infrastructure investment can be considered representing traditional as well as climate-related infrastructure. In our setup, the government can also use public capital for adaptation and for mitigation and chooses the split between these three competing uses optimally.

Formally, the model gives rise to an optimal control problem of finite horizon consisting of a dynamic system with five-dimensional state vector representing the stocks of private capital, green capital, public capital, stock of brown energy in the ground, and emissions. The control vector is eight-dimensional, since it also comprises the split of public capital into mitigation, adaptation and infrastructure as time-dependent control functions excluding the choice of split for public capital mentioned earlier.

We characterize the optimal tax and investment policies for the government and examine the resultant paths of important macroeconomic variables, particularly, of those related to energy transition, CO<sub>2</sub> emission, and resource extraction. The complexity of the problem, however, necessitates both an analytical approach as well as the use of numerical methods.

Solving such a model of finite horizon poses the challenge to show that the turnpike properties are not violated and the trajectories of the finite horizon model can approximate the solution of the infinite horizon case. The turnpike property usually follows from imposing terminal state conditions which represent the stationary solution of the necessary optimality conditions. In our case the turnpike property follows from additional bound constraints of the capital assets. For generic studies of turnpike properties of such models, see also Faulwasser et al. (2020) and Grüne et al. (2021).

These numerical solutions allow us to investigate the optimal sequence of climate policy decisions with respect to infrastructure, mitigation and adaptation. In all cases considered in the paper, numerical solutions from our finite-horizon set up recover the turnpike property that is characteristics of the infinite horizon models. In terms of climate policy response, in our model, we find that the optimal policy can keep the CO<sub>2</sub> emission bounded for a wide-range of initial conditions of capital

stocks and  $\text{CO}_2$  levels. Specifically, we consider a scenarios with a high level of capital stocks and high level of  $\text{CO}_2$ .

The remaining part of the paper is organized as follows. Section 2 describes the optimal control model of climate change. In Sect. 3, we introduce the temperature dynamics which is not contained in the basic model. In Sect. 4 we discuss the necessary optimality conditions for the control problem with control and state constraints. Section 5 presents the numerical solution method and reports the results from several scenarios concerning, in particular, bounds on the  $\text{CO}_2$  emission. In Sect. 6, we consider two objectives arising from two different elasticity exponents in the welfare functional. We compute the Pareto front in two scenarios. Optimization over the Pareto front provides us with suitable weights for the two objectives. Section 7 concludes.

## 2 Optimal control model of climate change

We extend the Nordhaus DICE type model to include the adverse effects of climate change with a view to study the optimal policies for mitigation and adaptation to climate change until a transition to fossil-fuel-free green energy is successful. The green energy capital is a perfect substitute for fossil fuel in production. The climate change is modeled as an adverse effect of increase in atmospheric  $\text{CO}_2$  concentration ( $M$ ) on utility. The mitigation efforts reduce the proportion of carbon in fossil fuel burned that escapes into the atmosphere as  $\text{CO}_2$ . In contrast, adaptation alleviates the harmful effects of higher atmospheric  $\text{CO}_2$  levels.

The government raises revenue ( $e_p$ ) which is used for direct, utility-enhancing services and provision of public (physical) capital/infrastructure ( $G$ ), with the possibility of some wastage. To analyze the issue of climate change, besides its traditional use for enhancing productive efficiency in the economy, we allow government to use public capital for mitigation and adaptation.

The output of the production process is given by

$$Y = (v_1 G)^\beta A(A_g K_g + A_u u)^\alpha (K_p)^\zeta \quad (1)$$

with  $A, A_g, A_u > 0$ ,  $\alpha, \beta, \zeta > 0$ , and  $\alpha + \beta + \zeta < 1$ .  $K_g$  is the stock of green capital,  $K_p$  is the stock of (private) physical capital, and  $v_1 \in (0, 1]$ , as mentioned above, is the fraction of public capital ( $G$ ) used for the traditional purpose of enhancing productive efficiency. Finally,  $u$  is the amount of fossil fuel resource extracted and used, measured in terms of its carbon ( $\text{CO}_2$ ) content.

The felicity (utility) function depends on four arguments (i) per-capita consumption  $C$ ; (ii) the per-capita amount of tax revenue ( $\alpha_2 e_p$ ,  $\alpha_2 \in [0, 1]$ ) used for direct welfare enhancement (e.g., healthcare); (iii) atmospheric concentration of  $\text{CO}_2$  ( $M$ ) above the long-run sustainable level, the industrial level; and (iv) the per-capita amount of public capital expenditure ( $v_2 G$ ,  $v_2 \in [0, 1]$ ) allocated to climate change adaptation. The optimal control model so defined then has five state variables:

$K_p$ : private physical capital per capita

$K_g$ : private green capital per capita  
 $G$ : public capital per capita  
 $M$ : CO<sub>2</sub> (GHG) concentration in the atmosphere  
 $R$ : non-renewable resource (fossil energy)  
 and the five basic control variables are

$i_p$ : investment in physical capital  
 $i_g$ : investment in green capital  
 $e_p$ : government's net tax revenue  
 $u$ : extraction rate from the non-renewable resource  
 $C$ : per capita consumption

In addition, we consider the following three allocations of public capital as control functions:

- $v_1$ : standard infrastructure
- $v_2$ : adaptation
- $v_3$ : mitigation

We emphasize that these allocations are not just parameters to be optimized but are considered as time-dependent control functions  $v_k = v_k(t)$ ,  $k = 1, 2, 3$ . The state and control variables are denoted by

$$X = (K_p, K_g, G, R, M) \in \mathbb{R}^5, \quad U = (i_p, i_g, e_p, u, C) \in \mathbb{R}^5, \quad v = (v_1, v_2, v_3) \in \mathbb{R}^3.$$

The time horizon  $t_f > 0$  (years) is finite. The dynamic system in  $[0, t_f]$  of the global model of climate change is given by

$$\dot{K}_p = i_p - (\delta_p + n)K_p, \tag{2}$$

$$\dot{K}_g = i_g - (\delta_g + n)K_g, \tag{3}$$

$$\dot{G} = \alpha_1 e_p - (\delta_G + n)G, \tag{4}$$

$$\dot{M} = \gamma u - c(M - \kappa \tilde{M}) - \theta(v_3 \cdot G)^\phi, \tag{5}$$

$$\dot{R} = -u, \tag{6}$$

with initial conditions:

$$X(0) = X_0 \tag{7}$$

that will be specified later. The control constraint for the extraction rate  $u$  is given by

$$0 \leq u(t) \leq u_{max} \quad \forall t \in [0, t_f]. \tag{8}$$

There are three potential uses of government revenues, as mentioned earlier. The amount  $\alpha_1 e_p$  is invested in public capital,  $\alpha_2 e_p$  provides direct utility, and  $(1 - \alpha_1 - \alpha_2)e_p$  is administrative expense/waste. Of the total public capital,  $G$ , a fraction  $v_1$  is the usual/traditional public capital that augments the productivity of the production process. Another fraction  $v_2$  is used for adaptation. The remaining fraction  $v_3$  is used for mitigation. Hence, the infrastructural and climate oriented allocations of public capital satisfy the constraints:

$$v_k(t) \geq 0, \quad v_1(t) + v_2(t) + v_3(t) = 1 \quad \forall t \in [0, t_f]. \tag{9}$$

Moreover, the system is subject to several control-state and pure state constraints. For defining a *resource constraint* we introduce the scalar function

$$c(X, U) = Y - C - i_p - i_g - e_p - u\psi R^{-\tau} - \frac{\chi_p}{2} \left( \frac{i_p}{K_p} - \delta_p - n \right) K_p - \frac{\chi_g}{2} \left( \frac{i_g}{K_g} - \delta_g - n \right)^2 K_g \tag{10}$$

and impose the *mixed control-state equality constraint*

$$c(X(t), U(t)) = 0 \quad \forall t \in [0, t_f]. \tag{11}$$

Note that the mixed constraint does not depend on the allocations  $v$ . In later computations we shall realize that we also need state constraints on the capital assets  $K_p, K_g, G$  and the CO<sub>2</sub> concentration  $M$ . We prescribe lower bounds for the capital assets as state inequality constraints,

$$K_p(t) \geq K_p^{min}, \quad K_g(t) \geq K_g^{min}, \quad G(t) \geq G^{min} \quad \forall 0 \leq t \leq t_f, \tag{12}$$

and an upper bound for the CO<sub>2</sub> concentration

$$M(t) \leq M^{max} \quad \forall 0 \leq t \leq t_f. \tag{13}$$

To handle these state constraints in a more convenient form we introduce the function

$$s(X) = (K_p^{min} - K_p, K_g^{min} - K_g, G^{min} - G, M - M^{max})^* \in \mathbb{R}^4 \tag{14}$$

and consider the following state inequality constraint

$$s(X(t)) \leq 0 \quad \forall t \in [0, t_f]. \tag{15}$$

Finally, note that our dynamics (5) for the evolution of carbon emission, generating the stock of carbon in the atmosphere, is slightly different from the Nordhaus' DICE model as proposed in Nordhaus (2017). Nordhaus defines emission dynamics as time varying fraction of net output (after damages) that causes a carbon emission flow, partly absorbed by the ocean, but augmented by land carbon emission, that produces a stock of atmospheric carbon. The latter, called also carbon budget, in turn is the main driver of the global temperature, creating in turn the economic damages as a fraction of output. In our case we see the emission dynamics driven by the

equation (5) with  $\kappa > 0$  a parameter allowing for a stationary stock of atmospheric carbon,  $\kappa\bar{M}$ , some equilibrium level of carbon concentration, a parametrization that also other literature has used. If now the quantity of emission is a policy target, as was in the Kyoto Protocol, then equation (5) would imply a stationary solution. On the other hand if temperature is a target, as in the Paris agreement, then our emission dynamics could be translated into a global temperature via equation (25) using that as a target; see below. The two base cases of policy targets can also be found in Nordhaus (2008, Chapter V), giving rise to a stationary behavior of the atmospheric stock of carbon.

Let us now introduce the welfare functional. Recall, the felicity (utility) function depends on (i) per-capita consumption  $C$ ; (ii) the per-capita tax revenue ( $v_2 e_p$ ,  $\alpha_2 \in [0, 1]$ ); (iii) atmospheric concentration of  $\text{CO}_2$  ( $M$ ); and (iv) the per-capita expenditure on adaptation ( $v_2 G$ ,  $v_2 \in [0, 1]$ ). The preferences of the representative household (or the policy maker) are

$$\int_0^{t_f} e^{-(\rho-n)t} \frac{1}{1-\sigma} \left\{ \left[ C(\alpha_2 e_p)^\eta \left( 1 - \exp(-\xi(v_2 G)^\omega) \frac{M - \kappa\tilde{M}}{\bar{M} - \kappa\tilde{M}} \right)^\varepsilon \right]^{1-\sigma} - 1 \right\} dt, \tag{16}$$

where  $\tilde{M}$  is the preindustrial level of atmospheric  $\text{CO}_2$  and  $\bar{M} > \kappa\tilde{M}$  is a high  $\text{CO}_2$  level, with  $\kappa\tilde{M}$  being the level that would not need any adaptation and is the long-run sustainable level. We have chosen the value  $\bar{M} = 4.5$  in Table 1.  $\rho > 0$  is the time rate of preference,  $n > 0$  is the rate of population growth,  $\sigma > 0$  is the inverse of the elasticity of intertemporal substitution and  $\eta \in [0, 1]$ ,  $\varepsilon \in [0, 1]$ ,  $\xi > 0$ ,  $\omega \in [0, 1]$ , and  $\kappa > 0$  are other parameters. The restrictions on parameters ensure that social expenditures and adaptation are utility enhancing with diminishing marginal utility and carbon emission that increase  $M$  reduce utility with increasing marginal disutility. As visible in our objective function we have not taken global temperature to measure the effect on welfare, but rather the stock of atmospheric carbon which appears to be easier to measure as driving variable for damages, see the simulations below. Note that for  $\sigma \geq 1$ , we only need  $\eta, \varepsilon > 0$ . Parameter values are given in Table 1.

This approach differs from other models that map emissions to temperature changes and then to reduced productivity-cum-output, see Nordhaus and Boyer (2000). The direct disutility approach better captures the wide ranging impacts of climate change that may include health impacts, ecological loss and heightened uncertainty, in addition to reduced productivity. Finally, note that the discount factor adjusts for the population growth rate  $n$  from the pure discount rate  $\rho$  as all values are normalized by the population per capita.

The optimal control problem (OCP) now consists in maximizing the welfare functional (16) subject to the dynamical constraints (2)-(7), the control constraints (8), (9), the mixed control-state constraint (11) and the pure state constraints (12) and (13). To obtain a more compact form of the optimal control problem we use the vector of state and control variables  $(X, U, v)$  introduced above to write the dynamical system (2)-(6) in the form

**Table 1** Parameter values

Parameter	Value	Definition
$\rho$	0.03	Pure discount rate
$n$	0.015	Population Growth Rate
$\eta$	0.1	Elasticity of transfers and public spending in utility
$\epsilon$	1.1	Elasticity of CO <sub>2</sub> concentration in (dis)utility
$\omega$	0.5	Elasticity of public capital used for adaptation in utility
$\sigma$	2	Intertemporal elasticity of instantaneous utility
$A$	1	Total factor productivity
$A_g$	1	Efficiency index of green capital
$A_u$	100	Efficiency index of the non-renewable resource
$\alpha$	0.05	Output elasticity of inputs, $(A_g K_g + A_u u)^\alpha$
$\beta$	0.1	Output elasticity of public infrastructure, $(v_1 G)^\beta$
$\psi$	0.1	Scaling factor in marginal cost of resource extraction
$\tau$	2	Exponential factor in marginal cost of resource extraction
$\delta_p$	0.1	Depreciation rate of physical capital
$\delta_g$	0.05	Depreciation rate of private capital
$\delta_G$	0.05	Depreciation rate of public capital
$\Omega_p$	$\in [5, 15]$	q-elasticity of investment spending on private capital
$\Omega_g$	$\in [5, 15]$	q-elasticity of investment spending on public capital
$\chi_p$	$\frac{1}{(\delta_p+n)\Omega_p}$	
$\chi_g$	$\frac{1}{(\delta_g+n)\Omega_g}$	
$\alpha_1$	0.3	Proportion of tax revenue allocated to new public capital
$\alpha_2$	0.7	Proportion of tax revenue allocated to transfers and public consumption
$\bar{r}$	0.07	World interest rate (paid on public debt)
$\tilde{M}$	2.5	Equilibrium concentration of CO <sub>2</sub>
$\kappa$	1.2	Atmospheric concentration stabilization ratio (relative to $\tilde{M}$ )
$\bar{M}$	4.5	Value in disutility term in welfare (16)
$\gamma$	0.9	Fraction of greenhouse gas emissions not absorbed by the ocean
$c$	0.01	Decay rate of greenhouse gases in atmosphere
$\kappa$	1.2	Atmospheric concentration stabilization ratio (relative to $\tilde{M}$ )
$\theta$	0.01	Effectiveness of mitigation measures
$\phi$	0.9	Exponent in mitigation term $(v_3 G)^\phi$

$$\dot{X}(t) = f(X(t), U(t), v(t)), \quad X(0) = X_0. \tag{17}$$

Furthermore, let us denote the integrand of the welfare functional by

$$f_0(X, U, v) = \frac{1}{1 - \sigma} \left\{ \left[ C(\alpha_2 e_p)^\eta \left( 1 - \exp(-\xi(v_2 G)^\omega) \frac{M - \kappa \tilde{M}}{\bar{M} - \kappa \tilde{M}} \right)^\epsilon \right]^{1-\sigma} - 1 \right\}. \tag{18}$$

Then the optimal control problem can be written in compact form as follows:

$$\text{Maximize}_{(U,v)} W(X, U, v) = \int_0^{t_f} e^{-(\rho-n)t} f_0(X(t), U(t), v(t)) dt \quad (19)$$

subject to the dynamical constraint (17) and the control and state constraints (8)-(15).

### 3 Temperature dynamics

So far, the optimal control problem does not involve the temperature  $T(t)$  at time  $t$  (measured in Kelvins), because the main focus was on the dynamics of the  $\text{CO}_2$  concentration  $M(t)$  which directly enters the welfare functional (18, 19). Due to the *energy balance model* in Roedel and Wagner (2011) the dynamic behavior of the temperature is closely related to that of the  $\text{CO}_2$  concentration  $M(t)$ . Hence, in this paper we compute the temperature  $T(t)$  as arising from the solution  $M(t)$  of the optimal control problem. We do not need the feedback loop from temperature increase to economic welfare, since the disutility of welfare (damage) caused by a high  $\text{CO}_2$  level is already incorporated.

We shall follow the presentation of the temperature model in Maurer et al. (2015) and Atolia et al. (2023). Some parameters in the model equations had been improved by discussions with Roedel (2012). The change of the average surface temperature  $T(t)$  is given by the equation

$$c_h \frac{dT}{dt} = S_E - H - F_N, \quad T(0) = T_0. \quad (20)$$

All magnitudes on the right side indicate annual averages. Hence, each time step  $\Delta t$  is exactly one year which expressed in seconds gives

$$\Delta t = 365 \cdot 24 \cdot 60 \cdot 60 [s] = 31536000 [s].$$

Therefore, the differential equation changes to

$$\dot{T} \equiv \frac{dT}{dt} = \frac{\Delta t}{c_h} (S_E - H - F_N), \quad T(0) = T_0. \quad (21)$$

The earth's surface is greatly covered by oceans. Its heat capacity is given by the numerical value  $c_h = 210652078 [J/(m^2 K)]$ , which follows from the identity  $c_h = 0.7 \rho_w c_w d$ , where  $\rho_w = 1027 [kg/m^3]$  is the density and  $c_w = 4186 [J/(kg K)]$  is the specific heat capacity of the sea water;  $d = 70 [m]$  describes the depth of the oceanic top layer where a mixing and thus a heat transport takes place. The factor 0.7 represents the proportion of sea water in the total surface of the earth. The unit of  $\frac{\Delta t}{c_h}$  is given by

$$\frac{s}{J/(m^2 K)} = s m^2 K/J = m^2 K/W,$$

from which it follows that  $\frac{\Delta t}{c_h} \approx 0.149707 [m^2 K/W]$ .  $S_E$  is the supplied sun energy,  $H$  the non-radiative energy flux and  $F_N = F_{\uparrow} - F_{\downarrow}$  the net flux of the terrestrial radiation.  $F_{\uparrow}$  complies with the Stefan–Boltzmann—law, which has the form

$$F_{\uparrow} = \varepsilon \sigma T^4 \tag{22}$$

with the relative emissivity  $\varepsilon = 0.95$  and the Stefan–Boltzmann—constant

$$\sigma = 5.67 \cdot 10^{-8} [W/(m^2 K^4)].$$

Furthermore, the flux ratio is  $F_{\uparrow}/F_{\downarrow} = 116/97$  and the difference is  $S_E - H = (1 - \alpha_1(T)) \frac{Q}{4}$  with the solar constant  $Q = 1367 [W/m^2]$  and the planetary albedo  $\alpha_1$ , which indicates how much energy is reflected back to space. The factor  $\frac{1}{4}$  is the ratio between the cross-sectional area  $\pi r_{\text{earth}}^2$  and the surface area  $4\pi r_{\text{earth}}^2$  of the earth, because it receives the sun’s radiation flux only on a hemisphere. The share of non-reflected sun energy is given by the differentiable function

$$1 - \alpha_1(T) = k_1 \frac{2}{\pi} \arctan\left(\frac{\pi(T - 293)}{2}\right) + k_2, \tag{23}$$

with constants  $k_1 = 5.6 \cdot 10^{-3}$  and  $k_2 = 0.1795$ .

A high concentration of greenhouse gases affects the temperature through the so-called radiative forcing, which describes the change of incoming and outgoing energy in the atmosphere. For carbon dioxide CO<sub>2</sub> we have

$$F = 5.35 \ln\left(\frac{M(t)}{M_o}\right) [W/m^2] \tag{24}$$

with the pre-industrial CO<sub>2</sub> concentration  $M_o$ . In Maurer et al. (2015) we have allowed for a *delay* in this equation, since a change in the concentration of CO<sub>2</sub> may not immediately affect a change in the temperature. However, in long term behavior the temperature is not much affected by such a (small) delay and thus delays will not be taken into account.

In summary, we obtain the following differential equation for the average surface temperature  $T$ ,

$$\dot{T}(t) = \frac{\Delta t}{c_h} \left( (1 - \alpha_1(T(t))) \frac{Q}{4} - \frac{19}{116} \varepsilon \sigma T(t)^4 + 5.35 \ln\left(\frac{M(t)}{M_o}\right) \right), T(0) = T_0, \tag{25}$$

where the unit on the right hand side is given by  $[m^2 K/W] \cdot (W/m^2) = [K]$ . In the following, we shall consider the initial temperature  $T(0) = 290$  which is approximately 1.5 degree Celsius above the pre-industrial level.

### 4 Maximum principle: necessary optimality conditions

We formulate the necessary conditions of the Maximum Principle for optimal control problems with state constraints; see Hestenes (1966); Pontryagin et al. (1964); Hartl et al. (1995); Maurer (1979) see also Atolia et al. (2023).

We use the direct-adjointing approach in Hartl et al. (1995) to define the augmented standard Hamiltonian and the current-value augmented Hamiltonian. The existence of regular multipliers associated with the constraints depends on the regularity of the constraints; see Hartl et al. (1995); Maurer (1979). The mixed control-state constraint (11) satisfies the regularity condition in view of

$$\frac{\partial c}{\partial U}(X(t), U(t)) \neq 0 \quad \forall t \in [0, t_f].$$

The 4 state constraints in (12, 13), resp., (15) are state constraints of *order one* and satisfy the regularity condition

$$\frac{\partial Y}{\partial(U, v)}(X(t), U(t), v(t)) \neq 0 \quad \forall t \in [0, t_f] \quad Y \in \{\dot{K}_p, \dot{K}_g, \dot{G}, \dot{M}\}.$$

The *standard Hamiltonian* is given by

$$H(X, \lambda, U, v) = \lambda_0 e^{-(\rho-n)t} f_0(X, U, v) + \lambda f(X, U, v). \tag{26}$$

Here,  $\lambda_0 \geq 0$  is a scalar multiplier and  $\lambda$  denotes the adjoint variable (row vector)

$$\lambda = (\lambda_1, \lambda_2, \lambda_3, \lambda_4, \lambda_5) = (\lambda_{Kp}, \lambda_{Kg}, \lambda_G, \lambda_M, \lambda_R).$$

To define the *augmented Hamiltonian* we use the *direct adjointing approach* (see Hartl et al. 1995; Maurer 1979, where the control-state constraint (11) and the pure state constraints (15) are directly adjointed to the Hamiltonian by multipliers:

$$\mathcal{H}(X, \lambda, \mu, U, v) = H(X, \lambda, U, v) + \mu_c c(X, U) + \mu_s s(X). \tag{27}$$

Here,  $\mu$  is the multiplier associated with the mixed constraint (11) and the state constraints (12):

$$\mu = (\mu_c, \mu_s), \quad \mu_s = (\mu_{Kp}, \mu_{Kg}, \mu_G, \mu_M) \in \mathbb{R}^4.$$

The discount factor  $e^{-(\rho-n)t}$  in the standard augmented Hamiltonian can be eliminated by considering the so-called *current-value* augmented Hamiltonian

$$\mathcal{H}^c(X, \lambda^*, \mu^*, U, v) = e^{(\rho-n)t} \mathcal{H}(X, \lambda, \mu, U, v). \tag{28}$$

The adjoint variable  $\lambda^*$  and the multiplier  $\mu^*$  are related to those of the standard Hamiltonian by

$$\lambda^*(t) = e^{(\rho-n)t} \lambda(t), \quad \mu^*(t) = e^{(\rho-n)t} \mu(t).$$

We assume that the control problem is *normal* and, hence, we can set  $\lambda_0 = 1$  in the standard Hamiltonians (26) and (27). It is well-known that the control problem is normal in case of a free terminal state. However, we are not able to show normality in the presence of control and state constraints.

Let  $(X, U, v)$  be an optimal solution of the optimal control (OCP) problem of maximizing the welfare (19) subject to the constraints (2)–(15). To formulate the maximum conditions for the controls we introduce the control set at time  $t$ :

$$\Omega(t) = \{(U, v) \in \mathbb{R}^8 \mid i_p(t), i_g(t), e_p(t) \geq 0, C(t) > 0, 0 \leq u(t) \leq u_{max}, v_k \geq 0 (k = 1, 2, 3), v_1(t) + v_2(t) + v_3(t) = 1, c(X(t), U) = 0\}. \tag{29}$$

Then the Maximum Principle asserts the existence of a piecewise continuous adjoint function  $\lambda : [0, t_f] \rightarrow \mathbb{R}^5$ , a continuous multiplier function  $\mu_c : [0, t_f] \rightarrow \mathbb{R}$  and a piecewise continuous multiplier functions  $\mu_s : [0, t_f] \rightarrow \mathbb{R}^4$  such that the following conditions hold for  $t \in [0, t_f]$ :

*Adjoint equation:*

$$\dot{\lambda}(t) = -\frac{\partial \mathcal{H}}{\partial X}(X(t), \lambda(t), \mu(t), U(t), v). \tag{30}$$

*Boundary conditions for adjoint variable:*

$$\lambda_i(t_f) s_i(X(t_f)) = 0, \quad i = 1, 2, 3, 4, \quad \lambda_R(t_f) = 0. \tag{31}$$

*Maximum conditions for controls:*

$$H(X(t), \lambda(t), \mu(t), U(t), v(t)) = \max_{(U,v) \in \Omega(t)} H(X(t), \lambda(t), U, v). \tag{32}$$

*Local maximum conditions when  $i_p(t), i_g(t), e_p(t), C(t) > 0$  and  $0 < u(t) < u_{max}$ :*

$$\frac{\partial \mathcal{H}}{\partial v}(X(t), \lambda(t), U(t), v(t)) = 0 \quad \text{for } v \in \{i_p, i_g, e_p, C, u\}. \tag{33}$$

*Complementary conditions:*

$$\mu_s(t) \geq 0, \quad \mu_s(t) s(X(t)) = 0 \quad \forall t \in [0, t_f]. \tag{34}$$

The adjoint variable  $\lambda$  and the multipliers  $\mu_c, \mu_s$  can be computed as the Lagrange multipliers of the nonlinear programming problem defined by the discretized control problem, see eg. Betts (2020); Büskens and Maurer (2000); Göllmann and Maurer (2014).

In Atolia et al. (2023) we have computed an (approximate) stationary solution of the canonical system and the maximum conditions. But here the analysis of stationary points of the necessary conditions is very complicated due to the presence of state constraints. Instead we can draw some information on stationary points from the turnpike behavior of the unconstrained solution; see Sect. 5.2. Note that in case of nonlinearities arising from the temperature dynamics one can also have multiple equilibria, see Greiner et al. (2010).

## 5 Numerical solutions

### 5.1 Discretization and nonlinear programming methods

We choose the numerical approach "First Discretize then Optimize" to solve the optimal control problem OCP defined in (1)–(19). The discretization of the control problem on a fine grid leads to a large-scale nonlinear programming problem (NLP) that can be conveniently formulated with the help of (AMPL), A MATHEMATICAL PROGRAMMING LANGUAGE, which was developed by Fourer et al. (1993). AMPL can be linked to several powerful optimization solvers. We use the Interior-Point Optimization Solver IPOPT; see Wächter and Biegler (2006). Details of discretization methods may be found in Betts (2020); Büskens and Maurer (2000); Göllmann and Maurer (2014). The following computations for the terminal time  $t_f = 200$  (years) are performed with  $N = 2000$  grid points using the trapezoidal rule as integration method. Choosing the error tolerance  $tol = 10^{-8}$  in IPOPT, we can expect that the state variables are correct up to 4 – 5 decimal digits. The Lagrange multipliers of the NLP yield approximations of the adjoint variables and multipliers of the optimal control problem which enables us to verify the necessary optimality conditions.

In the following computations, we fix the initial conditions  $X(0)$ ,

$$K_p(0) = 2.5, K_g(0) = 0.3, G(0) = 0.8, M(0) = 3.25, R(0) = 1, T(0) = 290, \quad (35)$$

and the large time horizon  $t_f = 200$  (years). The  $CO_2$  concentration  $M(0) = 3.25$  is rather high and the initial temperature  $T(0) = 290$  (Kelvin) is 1.5 degree above the pre-industrial temperature. These initial conditions mirror approximatively the actual data.

### 5.2 Solutions with free terminal state $X(t_f)$

First we analyse the control problem with a free terminal state  $X(t_f)$ . We obtain the following numerical results for the objective value (welfare) and terminal state variables

$$W(U, v) = -19.22 : K_p(t_f) = 0.8352, K_g(t_f) = 0.1314, G(t_f) = 0.5536, \\ M(t_f) = 3.279, R(t_f) = 0.09956, T(t_f) = 292.46, \quad (36)$$

The negative value of the welfare is due to the negative scaling factor  $1 - \sigma = -1$  in the welfare functional (16). The control and state trajectories are displayed in Fig. 1. The  $CO_2$  concentration reaches the rather high value  $M(t) = 3.48$  at  $t = 110$ . This is responsible for the high temperature value  $T(t) = 292.8$  at  $t = 127$  which is 2.8 deg. above the initial temperature  $T(0) = 290$ . Though in the long run the concentration  $M$  comes down to  $M = 3.27$  close to the initial value value  $M(0) = 3.25$ , the temperature settles at the high value  $T(t_f) = 292.4$ . The mitigation effort  $v_3(t)$  is still very small. The extraction rate  $u(t)$  is so high that it nearly depletes the resource  $R$ . We also observe that the capital assets  $K_p, K_g, G$  dramatically decrease during a terminal

period while the consumption is increasing. This behavior is typical for economic finite-horizon optimal control problems without terminal constraints. Hence, in the following we impose suitable terminal inequality constraints in the form of state constraints (14) and (15) for the capital assets:

$$K_p(t) \geq 2.2, \quad K_g(t) \geq 0.3, \quad G(t) \geq 0.8. \tag{37}$$

### 5.3 Solution for state constraint $M(t) \leq 3.3$ for $t \in [0, 200]$

Now we consider the solution under the state constraints (37) for the capital assets, and impose the bound  $M(t) \leq 3.3, 0 \leq t \leq 200$ , for the  $CO_2$  concentration. We get the following numerical results for the welfare and terminal state variables:

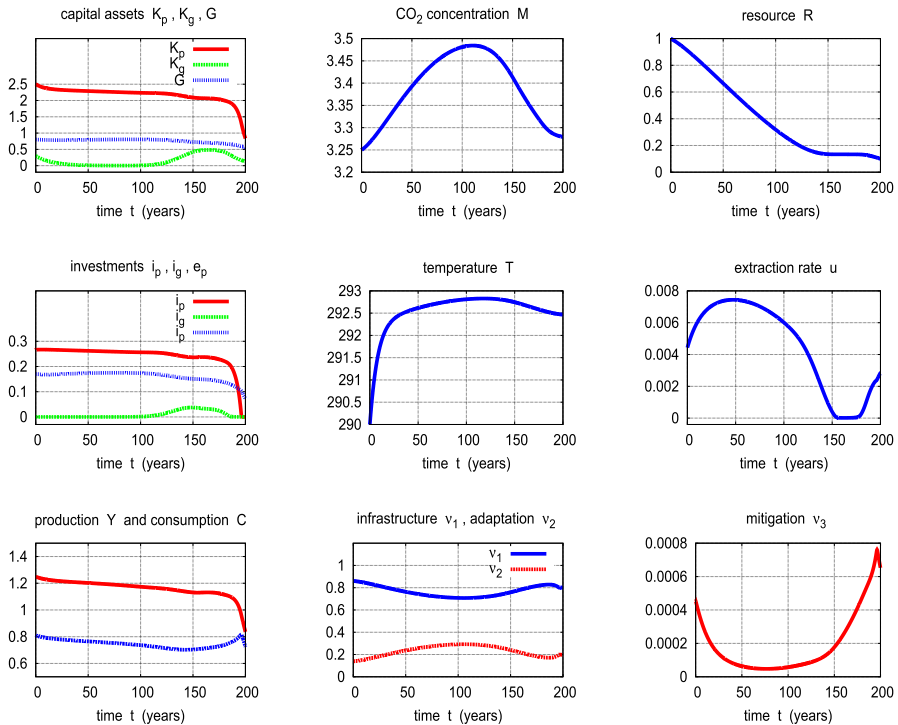


**Fig. 1** State and control trajectories for terminal time  $t_f = 200$  and initial states (35) and free terminal state  $X(t_f)$ . *Top row:* (left) physical capital  $K_p$ , green capital  $K_g$  and government capital  $G$ , (middle)  $CO_2$  concentration  $M$ , (right) resource  $R$ . *Middle row:* (left) investments  $i_p$  and  $i_g$  and tax revenue  $e_p$ , (middle) temperature  $T$ , (right) extraction rate  $u$ . *Bottom row:* (left) consumption  $C$  and productivity  $Y$ , (middle) infrastructure  $v_1$ , (right) adaptation  $v_2$  and mitigation  $v_3$

$$W(U, \nu) = -20.96 : K_p(t_f) = 2.2, K_g(t_f) = 0.3, G(t_f) = 0.8, M(t_f) = 3.3, R(t_f) = 0.8624, T(t_f) = 292.5, \tag{38}$$

The control and state trajectories are displayed in Fig. 2.

The capital assets  $K_p, K_g, G$  exhibit a turnpike behavior and stay on the boundary of the state constraints (37) for most of the time. Also, the  $CO_2$  concentration  $M$  has a boundary arc  $M(t) = 3.3$  for  $t \geq 32$  except for a small terminal interval. The temperature settles at  $T(t) = 292.5$  for  $t \geq 50$ . The high temperature motivates us to enforce a more restrictive bound for  $M(t)$  at least on the terminal part of the planning period.

### 5.4 Solution for state constraint $M(t) \leq 3.0$ for $t \in [40, 200]$

We require that the  $CO_2$  concentration stay below the value  $M = 3.0$  for  $t \geq 40$ . We get the following numerical results for the welfare and terminal state variables:

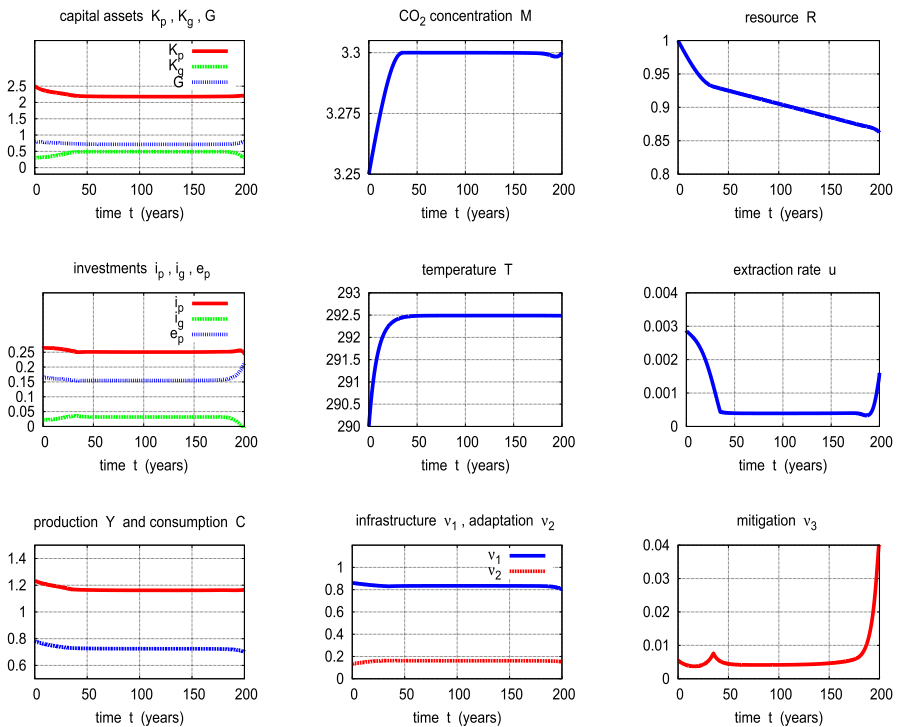


**Fig. 2** State and control trajectories for terminal time  $t_f = 200$ , initial states (35), state constraints (37) and state constraint  $M(t) \leq 3.3$ . *Top row:* (left) physical capital  $K_p$ , green capital  $K_g$  and government capital  $G$ , (middle)  $CO_2$  concentration  $M$ , (right) resource  $R$ . *Middle row:* (left) investments  $i_p$ , and  $i_g$  and tax revenue  $e_p$ , (middle) temperature  $T$ , (right) extraction rate  $u$ . *Bottom row:* (left) consumption  $C$  and productivity  $Y$ , (middle) infrastructure  $v_1$  and adaptation  $v_2$ , (right) mitigation  $v_3$

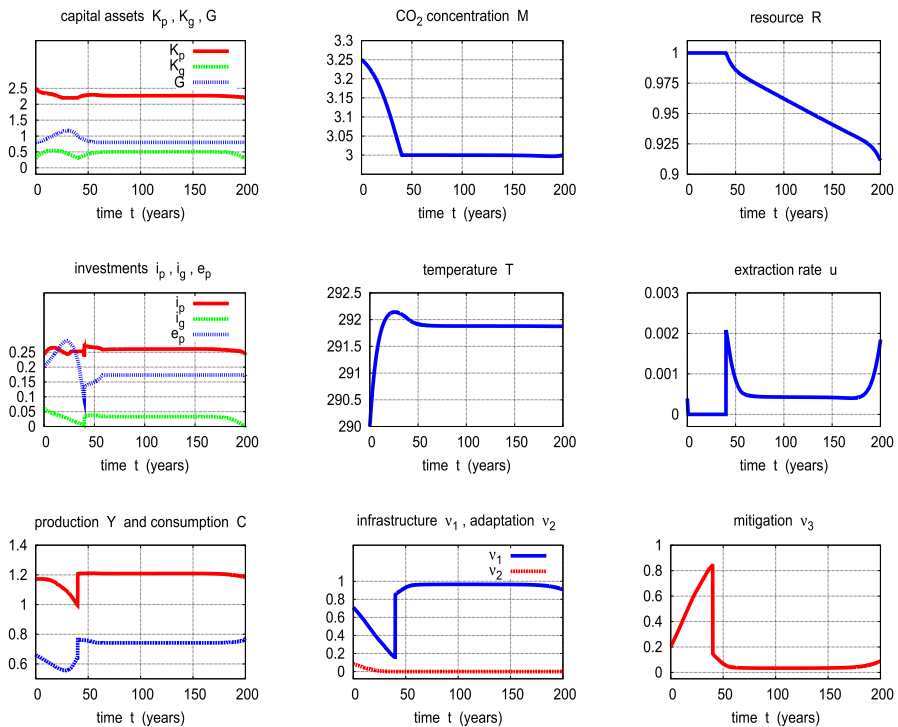
$$W(U, v) = -24.93 : K_p(t_f) = 2.2, K_g(t_f) = 0.3, G(t_f) = 0.8, M(t_f) = 3.0, R(t_f) = 0.9112, T(t_f) = 291.87. \tag{39}$$

Figure 3 shows the control and state trajectories.

The CO<sub>2</sub> concentration  $M$  stays on the boundary  $M(t) = 3.0$  for  $t \geq 40$  except on a small terminal interval. The temperature comes down to  $T(t_f) \leq 292$  after a short overshoot. To reach the goal of a smaller CO<sub>2</sub> concentration the extraction rate  $u(t)$  decreases significantly so that the resource  $R$  is far from being exhausted. Nevertheless, the welfare  $W(X, U, v)$  is not much smaller than in the previous cases.

### 5.5 Solution for state constraint $M(t) \leq 2.6, \forall t \in [50, 200]$

This very restrictive constraint leads to the solution shown in Fig. 4. Numerical results for the welfare and the terminal state variables are



**Fig. 3** State and control trajectories for terminal time  $t_f = 200$ , initial states (35), state constraints (37) and state constraint  $M(t) \leq 3.0$ . *Top row:* (left) physical capital  $K_p$ , green capital  $K_g$  and government capital  $G$ , (middle) CO<sub>2</sub> concentration  $M$ , (right) resource  $R$ . *Middle row:* (left) investments  $i_p$ , and  $i_g$  and tax revenue  $e_p$ , (middle) temperature  $T$ , (right) extraction rate  $u$ . *Bottom row:* (left) consumption  $C$  and productivity  $Y$ , (middle) infrastructure  $v_1$  and adaptation  $v_2$ , (right) mitigation  $v_3$

$$W(U, v) = -40.99 : K_p(t_f) = 2.2, K_g(t_f) = 0.3, G(t_f) = 0.8, \\ M(t_f) = 2.6, R(t_f) = 0.9236, T(t_f) = 291.87, \tag{40}$$

The  $CO_2$  concentration is steered down to  $M(t) \leq 2.6$  on  $[50, 200]$ . This has the effect that the temperature remains below  $T = 291$  on  $[50, 200]$  which is only 1 deg. higher then the initial temperature. However, it can not be avoided that the temperature reaches the high value  $T(t) = 292.0$  already at  $t = 20$ . The exhaustion rate  $u(t)$  is nearly zero on  $[0, 50]$  and remains on a small level which causes the high level  $R(t_f) = 0.9236$  of the terminal resource. The small exhaustion rate is also responsible for the low production and consumption for  $t \leq 50$ . Mitigation measures are dominant on  $[0, 50]$  and push adaptation and infrastructure aside.

It is interesting to note that we obtain a similar solution by imposing the following state constraint on the temperature:

$$T(t) \leq T_{max} = 291 \quad \forall 50 \leq t \leq 200. \tag{41}$$

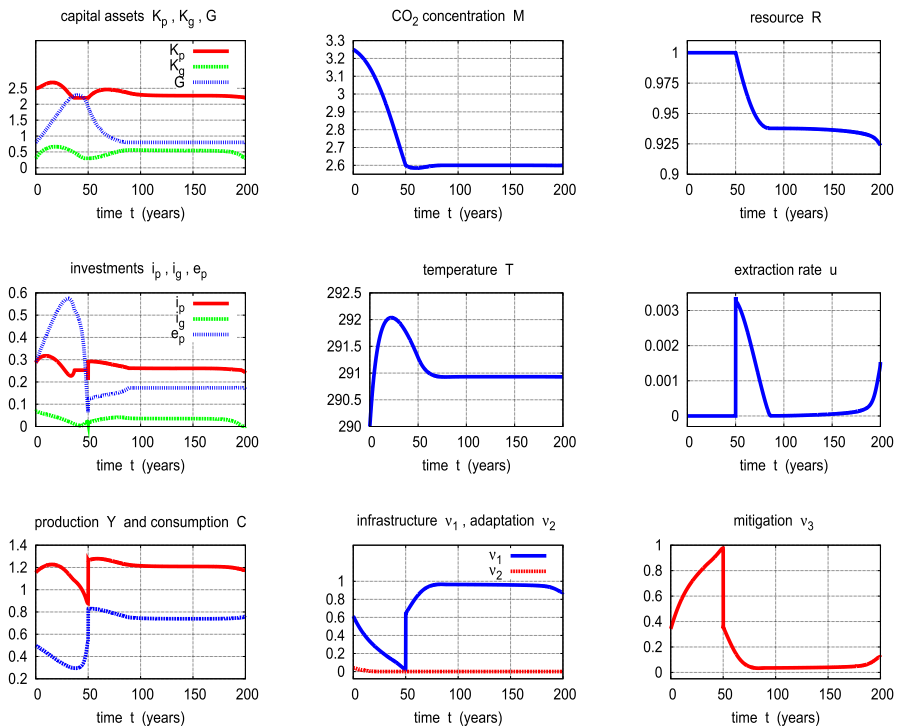


**Fig. 4** State and control trajectories for terminal time  $t_f = 200$ , initial states (35), state constraints (37) and state constraint  $M(t) \leq 2.6$ . *Top row:* (left) physical capital  $K_p$ , green capital  $K_g$  and government capital  $G$ , (middle)  $CO_2$  concentration  $M$ , (right) resource  $R$ . *Middle row:* (left) investments  $i_p$ , and  $i_g$  and tax revenue  $e_p$ , (middle) temperature  $T$ , (right) extraction rate  $u$ . *Bottom row:* (left) consumption  $C$  and productivity  $Y$ , (middle) infrastructure  $v_1$  and adaptation  $v_2$ , (right) mitigation  $v_3$

## 6 Multi-objective approach to the optimal control problem under state constraints

The simultaneous optimization of multi-objective functions results in a set of trade-off or Pareto solutions. Although there is a wealth of literature involving finite-dimensional optimization problems (see Eichfelder 2008), only a few papers are devoted to optimal control problems; see, eg., Kaya and Maurer (2014) and Eichfelder et al. (2023). The problem of optimizing over the Pareto front of a bi-objective control problem has recently been addressed by Kaya and Maurer (2023).

In this section, we study a bi-objective optimal control problem which arises from the fact that the control system and the objectives depend on some parameters which have significant impact on the solution but which can not be estimated precisely. One such critical parameter is the elasticity  $\epsilon$  of the  $CO_2$  concentration describing the disutility in the objective (16), resp., (19). There we have chosen the nominal value  $\epsilon = 1.1$ . Let us denote the welfare function by  $W(X, U, v, \epsilon)$  to underline its dependence on  $\epsilon$ . We shall compare the welfare  $W(X, U, v, \epsilon)$  for the small parameter  $\epsilon_1 = 0.6$  and for the large parameter  $\epsilon_2 = 1.8$ . Our focus is on the trade-off between the solutions for the functionals

$$F_k(X, U, v) = W(X, U, v, \epsilon_k), \quad k = 1, 2. \quad (42)$$

To generate the Pareto front for this bi-objective optimal control problem we apply the weighted sum scalarisation and thus *maximize* the following weighted sum functional with weight  $w \in [0, 1]$ :

$$F_w(X, U, v) = (1 - w) \cdot F_1(X, U, v) + w \cdot F_2(X, U, v). \quad (43)$$

Standard homotopy methods are used to compute the solution for weights

$w_i = i/N$ ,  $i = 0, \dots, N$ , with, eg.,  $N = 100$ . Denote the state and control solution depending on the weight  $w$  by  $X^w(\cdot)$ ,  $U^w(\cdot)$ ,  $v^w(\cdot)$  and the objectives values by  $F_1^w$  and  $F_2^w$ . Then the Pareto front is defined the by curve  $PF = \{ (F_1^w, F_2^w) \mid w \in [0, 1] \}$ .

### 6.1 Pareto front for state constraints (37) and $M(t) \leq 3.3$

The Pareto front is *concave* as shown in Fig. 5a since we are *maximizing*. We noted earlier that the objective values are negative.

Now let us determine the point where the Pareto front has *minimal distance* to the origin. To this end we have to minimize the so-called master function

$$F_m(w) = \|(F_1^w, F_2^w)\|_2. \quad (44)$$

By inspecting the numerical results of maximizing the weighted objective (43) we see that the minimum of the function  $F_m(w)$  is attained at  $w = w_{opt} = 0.58$ , depicted in Fig. 5b, with functional value  $F(w_{opt}) = 28.94$ . Solving the optimal control problem (43) with weight  $w = w_{opt} = 0.58$  we obtain

$$F_w(X, U, v) = -19.64, \quad M(t_f) = 3.3, \quad T(t_f) = 292.49.$$

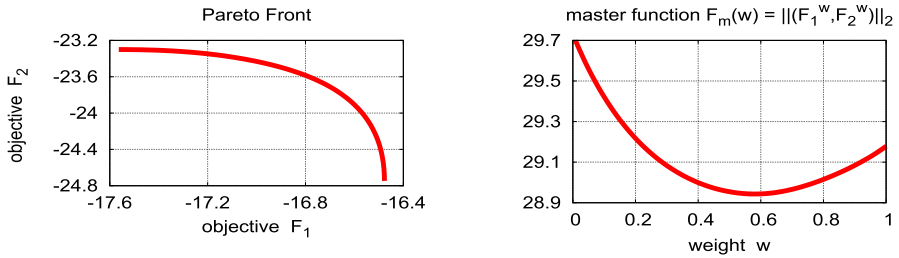


**Fig. 5** Pareto front for functionals  $F_1, F_2$  under state constraints (37) and  $M(t) \leq 3.3, 0 \leq t \leq 200$ . **a** Pareto front  $\{ (F_1^w, F_2^w) \mid w \in [0, 1] \}$ , **b** Master function  $F_m(w) = \|(F_1^w, F_2^w)\|_2$  for  $0 \leq w \leq 1$ .

The control and state trajectories are very close to those in Fig. 2 and are not shown here.

Instead of using the weighed-sum scalarization (43) we can implement the Chebyshev scalarization described in Kaya and Maurer (2014, 2023). This amounts to maximizing the non-smooth objective

$$F_w(X, U, v) = \max \{ (1 - w) \cdot F_1(X, U, v), w \cdot F_2(X, U, v) \}, \quad 0 \leq w \leq 1. \tag{45}$$

This approach allows to optimize a *master function* like (44) in a more systematic way using bisection of gradient-like methods.

### 6.2 Pareto front for state constraints (37) and $M(t) \leq 2.6, 50 \leq t \leq 200$

Again, the Pareto front is *concave* as shown in Fig. 6a.

The minimum of the master function  $F_m(w) = \|(F_1^w, F_2^w)\|_2$  is attained at  $w = w_{opt} = 0.52$ . The corresponding control and state trajectories are rather close to those in Fig. 4 and can be regarded as a compromise solution.

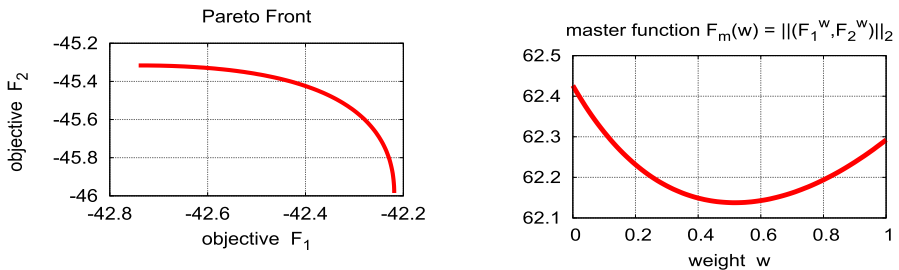


**Fig. 6** Pareto front for functionals  $F_1, F_2$  under state constraints (37) and  $M(t) \leq 2.6, 50 \leq t \leq 200$ . **a** Pareto front  $\{ (F_1^w, F_2^w) \mid w \in [0, 1] \}$ , **b** Master function  $F_m(w) = \|(F_1^w, F_2^w)\|_2$  for  $0 \leq w \leq 1$ .

## 7 Conclusions

Climate change and rising climate risks currently pose great challenges for academic work as well as policymakers. Those challenges are recently not only not to surpassing upper limits of atmospheric  $CO_2$  concentration, but reducing the atmospheric concentration and excessive temperature rise, generating increasing weather extremes. We propose an optimal control model of climate control including eight control variables and five state variables that are subject to a rather complex mixed control-state constraints. Besides the more standard control variables (consumption, investments in capital goods, extraction of nonrenewable resource) we propose an extensive dynamic model with three allocations of public capital (infrastructure, adaptation and mitigation) as time-dependent control objectives and five economic state variables.

Such an attempt not only needs to analyze the necessary optimality conditions and computed steady state values evaluated by the current-value Hamiltonian but in particular the numerical evaluation through numerical procedures. For the numerical solution paths we have chosen a rather large time horizon of  $t_f = 200$  years, where we have computed numerical solutions in several scenarios using discretization and nonlinear programming methods. In all scenarios, the solutions exhibit a turnpike behavior. The main focus in our model is on the evolution of the  $CO_2$  concentration and a dynamic equation of the temperature (see Kaya and Maurer 2023) to measure the effect of the changing  $CO_2$  concentration on the temperature. This way either the carbon emission and concentration or the temperature can be used as policy target - since one can be converted into the other.

We first explore for  $t_f = 200$  the paths of the variables without state constraints, so the final outcomes to let the variables developing freely which is not a very satisfactory path for the control of the state variables—the  $CO_2$  emissions and temperature go to high levels—generates not the controls, such as infrastructure, adaptation, mitigation, shown in Fig. 1. Next we constrain the  $CO_2$  emission by an upper magnitude of 3.3 which gives the path of  $CO_2$ . The  $CO_2$  emission goes to an upper bound in a finite time, after 50 steps, and the extraction of the fossil fuel resources decline. Those paths correspond to appropriate controls, shown in Fig. 2. This is achieved with the value of the welfare function  $W = -20.96$ .

In the next scenario, Fig. 3, we constrain the  $CO_2$  emission to be not greater than the level 3, which gives us also the maximum temperature rise. Those results can also be achieved by the appropriate controls, in particular the fossil fuel extraction rate and welfare of  $W = -24.93$ , to a lower welfare than in the previous case. The next scenario is depicted in Fig. 4, with the  $CO_2$  constraint  $M(t) \leq 2.6$  for all  $t \in [50, 200]$ . This allows also the temperature to be constrained below previous cases, namely to  $T(t) \leq 291$  for all  $t \in [50, 200]$ . The welfare is now decreased as well:  $W = -40.99$ .

In general, we provide some dynamic estimates of how the scaling up of efforts of mitigation and adaptation can be funded and how the funds should be allocated between (traditional and climate related) infrastructure investment, mitigation and adaptation efforts. We find that infrastructure investment efforts are in most cases high, sometimes occurring with a delay effect. Since in this context successful mitigation policy means phasing in of renewable energy (see also Maurer and Semmler 2015) we have also explored what amount of traditional fossil energy should be left in situ in order to satisfy some  $CO_2$  emission and temperature constraints. Yet, our control actions might not work if we are high above the  $CO_2$  target, namely if there are—as demonstrated in simpler models by Greiner et al. (2010) and Nordhaus (2008)—tipping points and thresholds beyond which the climate and whether extremes accelerate. For a model proposing also other means of financing climate policies, for example climate bonds, see Orlov et al. (2018). Addressing these issues required enlarging and solving for higher dimensional nonlinear control problems. We also showed that our numerical solutions for finite horizon decision model have turnpike properties similar to infinite horizon models.

We also demonstrated why our multi-objective control approach should be complemented by the computation of a Pareto front that helps us to attach certain weights for the objectives in the objective functional. As we demonstrated we can then suggest a certain compromise between the perception of higher and lower risk of damages.

**Acknowledgements** We thank Tato Khundadze for valuable assistance. We also want to thank Manoj Atolia and Prakash Loungani for cooperation on the issues addressed in this paper.

**Funding** Open access funding provided by International Institute for Applied Systems Analysis (IIASA).

**Open Access** This article is licensed under a Creative Commons Attribution 4.0 International License, which permits use, sharing, adaptation, distribution and reproduction in any medium or format, as long as you give appropriate credit to the original author(s) and the source, provide a link to the Creative Commons licence, and indicate if changes were made. The images or other third party material in this article are included in the article's Creative Commons licence, unless indicated otherwise in a credit line to the material. If material is not included in the article's Creative Commons licence and your intended use is not permitted by statutory regulation or exceeds the permitted use, you will need to obtain permission directly from the copyright holder. To view a copy of this licence, visit <http://creativecommons.org/licenses/by/4.0/>.

## References

- Atolia M, Loungani P, Maurer H, Semmler W (2023) Optimal control of a global model of climate change with adaptation and mitigation. *Math Control Related Fields* 13:583–604. <https://doi.org/10.3934/mcrf.2022009>
- Betts JT (2020) Practical methods for optimal control and estimation using nonlinear programming. 3rd edition, *Advances in Design and Control*, SIAM Publications, Philadelphia <https://doi.org/10.1137/1.9780898718577>
- Bonen T, Loungani P, Semmler W, Koch S (2016) Investing to mitigate and adapt to climate change: a framework model. IMF working paper WP no 16/164, International Monetary Fund, Washington

- Büskens C, Maurer H (2000) SQP-methods for solving optimal control problems with control and state constraints: adjoint variables, sensitivity analysis and real-time control. *J Comput Appl Math* 120:85–108
- Eichfelder G (2008) Adaptive scalarization methods in multiobjective optimization. Springer, Vector Optimization
- Eichfelder G, Grüne L, Krüger L, Schießl J (2023) Relaxed dissipativity assumptions and a simplified algorithm for multiobjective MPC. *Comput Optim Appl* 86:1081–1116. <https://doi.org/10.1007/s10589-022-00398-4>
- Faulwasser T, Grüne L (2020) Turnpike properties in optimal control: an overview of discrete-time and continuous-time results. *arXiv arXiv:2011.13670*
- Fourer F, Gay DM, Kernighan BW (1993) AMPL: a modeling language for mathematical programming. Duxbury Press, Brooks-Cole Publishing Company
- Göllmann L, Maurer H (2014) Theory and applications of optimal control problems with multiple time-delays. *J Ind Manag Optim* 10:413–441
- Greiner A, Grüne L, Semmler W (2010) Growth and climate change: threshold and multiple equilibria. In: Crespo Cuaresma J, Palokangas T, Tarasyev A (eds) *Dyn Syst Econ Growth Environ*. Springer, Heidelberg and New York, pp 63–78
- Grüne L, Müller MA, Kellet CM, Weller SR (2021) Strict dissipativity for discrete discounted optimal control problems. *Math Control Related Fields* 11:771–796
- Hartl RF, Sethi SP, Vickson RG (1995) A survey of the maximum principles for optimal control problems with state constraints. *SIAM Rev* 37:181–218
- Hestenes M (1966) *Calculus of variations and optimal control theory*. Wiley, New York
- Kaya CY, Maurer H (2014) A numerical method for nonconvex multi-objective optimal control problems. *Comput Optim Appl* 57(685–702):2013. <https://doi.org/10.1007/s10589-013-9603-2>
- Kaya CY, Maurer H (2023) Optimization over the Pareto front of nonconvex multi-objective optimal control problems. *Comput Optim Appl* 86:1247–1274. <https://doi.org/10.1007/s10589-023-00535-7>
- Global Warming of 1.5 °C. Intergovernmental Panel of Climate Change (2018)
- Maurer H (1979) On the minimum principle for optimal control problems with state constraints. *Rechenzentrum der Universität Münster, Report 41*, Münster
- Maurer H, Preuß JJ, Semmler W (2015) Policy scenarios in a model of optimal economic growth and climate change. Chapter 5 : *The Oxford Handbook of the Macroeconomics of Global Warming*, (eds. Bernard, L. Semmler, W.), Oxford University Press
- Maurer H, Semmler W (2015) Expediting the transition from non-renewable to renewable energy via optimal control. *Discrete Contin Dyn Syst* 35:4503–4525
- Nordhaus W (2008) *The question of balance*. Yale University Press, New Haven
- Nordhaus WW (2017) Revisiting the social cost of carbon. *PNAS* 114:1518–1523
- Nordhaus W, Boyer J (2000) *Warming the World. Economic models of global warming*. Cambridge: MIT-Press, Cambridge
- Orlov S, Rovenskaya E, Semmler W, Puauschunder J (2018) Green bonds, transition to a low-carbon economy, and intergenerational fairness: Evidence from an extended DICE model. *IIASA Working Paper, WP-18-001*
- Pontryagin LS, Boltyanski VG, Gramkrelidze RV, Miscenko EF (1964) *The mathematical theory of optimal processes*. Brown, A Pergamon Press Book, The Macmillan Company, New York, Translated by D.E
- Roedel W (2012) Private communication
- Roedel W, Wagner T (2011) *Physik Unserer Umwelt: Die Atmosphäre*. Springer, Berlin
- Wächter A, Biegler LT (2006) On the implementation of an interior-point filter line-search algorithm for large-scale nonlinear programming. *Math Program* 106:25–57

**Publisher's Note** Springer Nature remains neutral with regard to jurisdictional claims in published maps and institutional affiliations.

## Authors and Affiliations

Helmut Maurer<sup>1</sup> · Willi Semmler<sup>2,3,4</sup> 

✉ Willi Semmler  
SemmlerW@newschool.edu

Helmut Maurer  
helmut.maurer@uni-muenster.de

<sup>1</sup> Institut für Analysis und Numerik, Universität Münster, Einsteinstr. 62, 48149 Münster, Germany

<sup>2</sup> Department of Economics, The New School, 6E 16th St, New York, NY 10003, USA

<sup>3</sup> University of Bielefeld, Bielefeld, Germany

<sup>4</sup> IIASA, Laxenburg, Austria